Published in final edited form as:
Arch Biochem Biophys. 2013 November 1; 539(1): . doi:10.1016/j.abb.2013.08.019.

Kinetic and pH Studies on Human Phenylethanolamine *N*-Methyltransferase

Qian Wu[1] and **Michael J. McLeish**[1,2,*]

[1]Department of Medicinal Chemistry, University of Michigan, 428 Church St, Ann Arbor, Michigan 48105

[2]Department of Chemistry and Chemical Biology, Indiana University-Purdue University Indianapolis, 402 N. Blackford St. Indianapolis, IN 46202

Abstract

Phenylethanolamine *N*-methyltransferase (PNMT) catalyzes the conversion of norepinephrine (noradrenaline) to epinephrine (adrenaline) while, concomitantly, S-adenosyl-L-methionine (AdoMet) is converted to S-adenosyl-L-homocysteine. This reaction represents the terminal step in catecholamine biosynthesis and inhibitors of PNMT have been investigated, *inter alia*, as potential antihypertensive agents. At various times the kinetic mechanism of PNMT has been reported to operate by a random mechanism, an ordered mechanism in which norepinephrine binds first, and an ordered mechanism in which AdoMet binds first. Here we report the results of initial velocity studies on human PNMT in the absence and presence of product and dead end inhibitors. These, coupled with isothermal titration calorimetry and fluorescence binding experiments, clearly shown that hPNMT operates by an ordered sequential mechanism in which AdoMet binds first. Although the log*V* pH-profile was not well defined, plots of log*V*/*K* versus pH for AdoMet and phenylethanolamine, as well as the pK_i versus pH for the inhibitor, SK&F 29661, were all bell-shaped indicating that a protonated and an unprotonated group are required for catalysis.

Keywords

mechanism; inhibition; ordered sequential; epinephrine; adrenaline; AdoMet

INTRODUCTION

Phenylethanolamine *N*-methyltransferase (PNMT; E.C. 2.1.1.28) catalyzes the terminal step in catecholamine biosynthesis, i.e., the conversion of norepinephrine (NE) to epinephrine (Epi) with the concomitant conversion of S-adenosyl-L-methionine (AdoMet) to S-adenosyl-L-homocysteine (AdoHcy) [1, 2] (Scheme 1). In addition to the high levels present in the adrenal medulla, Epi makes up 5–10% of the total catecholamine content of the brain. However, its function within the central nervous system (CNS) is not well understood [3]. CNS Epi has been implicated in a variety of activities including central control of blood

Corresponding author: Michael J. McLeish, Department of Chemistry and Chemical Biology, Indiana University-Purdue University Indianapolis, 402 N. Blackford St, Indianapolis IN 46202, Tel: +1 317 274 6889, Fax: +1 317 274 4701, mcleish@iupui.edu, Web: www.chem.iupui.edu/people/michael-j-mcleish.

pressure and respiration [4, 5], secretion of hormones from the pituitary [6], activation of the K_1-adrenoceptor [7] and may even be responsible for some of the neurodegeneration found in Alzheimer's disease [8, 9]. In light of this multitude of apparent activities considerable effort has been expended in obtaining inhibitors of PNMT that could be used to delineate the role of central Epi and even may be of pharmaceutical benefit [10–17].

The majority of the initial studies on PNMT inhibitors used partially purified homogenates of adrenal glands from a variety of sources including monkey [2], rabbit [18, 19], rat [20], bovine [21] and human [22]. It took more than thirty years for human PNMT (hPNMT) to be cloned, expressed in *E. coli* and purified to homogeneity [23]. The purified enzyme was used to show that structure-activity models derived from inhibition of the bovine enzyme were likely to hold true for the human isozyme (hPNMT) [24, 25]. The availability of large quantities of purified enzyme also enabled the crystallization of hPNMT [26] and, over the past several years, X-ray structures have been obtained of hPNMT in complex with a number of substrates and inhibitors [27–32]. In each case the complex also contained either AdoMet or AdoHcy. The hPNMT complexes comprised the core class I AdoMet-dependent methyltransferase fold [33, 34], along with a cap containing around 40% of the residues, that interacts with the substrates/inhibitors and which completely covers the active site [27] (Figure 1A). At present it is not clear how substrates/inhibitors access the active site but it appears that a conformational change will be required. This may occur through movement of cap to completely expose the active site, or movement of a flexible loop that blocks one end of the site [27]. Further evidence suggestive of conformational changes is provided by studies showing synergism in both substrate and inhibitor binding [30].

Over the years there were several studies aimed at understanding the kinetic mechanism of PNMT. It was established rapidly that the reaction was irreversible, and was subject to product inhibition by both Epi [35] and AdoHcy [36]. Connett and Kirshner [21] suggested that, for bovine PNMT, both substrates could bind randomly, but that AdoMet was kinetically preferred. Conversely, Pohorecky and Baliga proposed that the rat enzyme operated by an ordered mechanism with norepinephrine binding first [20]. Pendleton and Snow [18] used inhibition studies to propose that the mechanism for rabbit PNMT was also ordered, but that AdoMet was the first substrate to bind. The latter observation was confirmed for several rabbit PNMT isozymes, but it was also noted that some abortive complexes were formed which could give rise to kinetic differences between isozymes [19, 37]. These proposed mechanisms were almost solely based on kinetic studies. In light of the variability of the conclusions, and the apparent differences between species, here we have used a combination of kinetic analysis, inhibition studies, isothermal titration calorimetry and fluorescence spectrophotometry to investigate the kinetic mechanism of human PNMT.

In recent times, the mechanism of the reaction catalyzed by PNMT has also been studied using computational approaches [38, 39]. The results showed that reaction took place via an S_N2 mechanism with methyl transfer being rate-limiting. The X-ray structure of the hPNMT:AdoHcy:NE complex [32] shows that two glutamic acid residues, Glu185 and Glu219, interact with the amine of NE, while an aspartic acid residue interacts with the hydroxyl group of the side-chain. It is thought that both glutamates will take part in catalysis, but the computational studies differ in their proposed roles for the two residues. In an attempt to clarify the issue we have determined the pH-rate profile for the overall reaction as well as the pH-profile for the binding of the inhibitor, SK&F 29661.

MATERIALS and METHODS

Materials

The wild-type hPNMT expression plasmid, pET17PNMT-his, was available from an earlier study [40]. Phenylethanolamine.HCl, octopamine.HCl, epinephrine.HCl, *S*-adenosyl-L-methionine and *S*-adenosyl-L-homocysteine were obtained through Sigma. [^{3}H]-*S*-Adenosyl-L-methionine (15 Ci/mmol) was from Moravek Biochemicals or Amersham Biosciences. SK&F 29661, SK&F 64139, LY134046, 3-trifluoromethyl phenylethanolamine (3-CF_3 PEA) and 7-nitro-1,2,3,4-tetrahydroisoquinoline (7-NO_2 THIQ) were available from a previous study as their hydrochloride salts [30]. All other buffers and reagents were the highest grade commercially available.

Assays of hPNMT Activity

Cell growth, expression and purification of hPNMT were performed as described previously [30]. The hPNMT-catalyzed reaction was followed by monitoring the transfer of a tritiated methyl group from [^{3}H]-AdoMet to phenylethanolamine (PEA) at 30 °C. A standard assay mixture contained potassium phosphate (50 mM, pH 8.0), PEA (200 M) and AdoMet including [^{3}H]-AdoMet (5 μM), in a total volume of 250 μL. For determination of kinetic constants, both substrate concentrations were varied between 0.3–3×K_m. Following the addition of enzyme, the reactions were incubated at 30 °C for 30 minutes, and then quenched by the addition of 0.5 M boric acid (500 μL, pH 10.0). Two milliliters of a mixture of toluene/isoamyl alcohol (7:3) were added, and the samples were vortexed for 30 seconds. The phases were separated by centrifugation and an aliquot of the organic phase (1 mL) was removed and added to 5 mL of scintillation fluid (Cytoscint, ICN). The radioactivity was quantitated by liquid scintillation spectrometry.

Initial velocity data were fitted to eq 1 for a sequential mechanism using SigmaPlot 9.0 (SPSS Inc.).

$$v=\frac{\mathrm{V[A][B]}}{K_{\mathrm{iA}}K_{\mathrm{b}}+K_{\mathrm{a}}[\mathrm{B}]+K_{\mathrm{b}}[\mathrm{A}]+[\mathrm{A}][\mathrm{B}]} \quad (1)$$

Here, in Cleland's nomenclature [41], [A] and [B] are substrate concentrations, K_{iA} is the dissociation constant for A, and K_a and K_b are the Michaelis constants (K_m values) for A and B, respectively.

Determination of inhibition constants (K_i values)

To obtain inhibition patterns the concentration of one substrate was fixed at its K_m value (5 μM and 100 μM for AdoMet and PEA, respectively). The concentration of the second substrate was then varied between 0.4–2.5×K_m at several fixed inhibitor concentrations (between 0–2.5×K_i). Depending on whether the inhibition patterns indicated competitive, non-competitive or uncompetitive inhibition the initial velocity data were then fitted to eqs 2–4 using SigmaPlot.

$$v=\frac{V_{\max}[S]}{[S]+K_{\mathrm{m}}\left(1+\frac{[I]}{K_{\mathrm{is}}}\right)} \quad (2)$$

$$v=\frac{V_{\max}[S]}{K_{\mathrm{m}}\left(1+\frac{[I]}{K_{\mathrm{is}}}\right)+[S]\left(1+\frac{[I]}{K_{\mathrm{ii}}}\right)} \quad (3)$$

$$v=\frac{V_{\max}[S]}{K_{\mathrm{m}}+[S]\left(1+\frac{[I]}{K_{\mathrm{ii}}}\right)} \quad (4)$$

In eqs 2–4, [S] is the concentration of the varied substrate, [I] is the inhibitor concentration and K_{is} and K_{ii} are the slope and intercept inhibition constants, respectively.

Isothermal Titration Calorimetry

A VP-ITC instrument from MicroCal, LLC (GE Healthcare) was used to measure the thermodynamic parameters of hPNMT binding to its substrates and/or inhibitors. The hPNMT was stored in a buffer containing 20 mM Tris (pH 7.2), 1 mM EDTA, 0.5 mM DTT, and 15% glycerol. Protein concentrations were determined using the Bradford method [42]. The protein solution was diluted in 50 mM potassium phosphate (pH 8.0) to the required concentration (25–200 μM) before being degassed and placed in the stirred calorimetric cell. In some cases AdoMet or AdoHcy was added to the protein solutions prior to degassing. Stock solutions of substrates and inhibitors were prepared by dissolving in water and the solution pH was adjusted to 8.0. The titration solutions were prepared by dilution of these stocks into 50 mM potassium phosphate (pH 8.0). An appropriate amount of enzyme storage buffer was added to match the buffer concentration in the stirred cell. After degassing the titration solution was placed in a 300 μL syringe. Generally, an initial injection of 10 μL was followed by 25–29 injections of 9.5 μL at 180 sec intervals. Controls for the heats of dilution and mixing were determined in separate experiments by titrations carried out in the absence of enzyme. These titrations were subtracted from the experimental analysis before the data were analyzed. The binding constants (K_{A}) were obtained by fitting data to a single-site model [43] using the Origin version 7.0 software supplied with the MicroCal instrument.

Fluorescence spectrophotometry

Fluorescence measurements were carried out in potassium phosphate buffer (50 mM, pH 8.0) at room temperature on a Fluoromax-2 (Jobin Yvon) fluorescence spectrophotometer. For all experiments, the excitation wavelength was 280 nm, and the emission spectra were recorded from 310 to 400 nm. The quartz fluorescence cuvettes used for the measurement of sample and blank spectra had a volume of 1 mL and a 10 mm path length. The enzyme concentration of the samples was 10 μg/mL. Stock solutions for compounds used in the fluorescence studies, AdoMet, AdoHcy, SK&F29661, SK&F64139, LY134046 were prepared as described above. Aliquots of the stock solution were added from low to high concentration to both the blank and sample, and the data were all corrected for dilution. Fluorescence data were fitted to the equation for a rectangular hyperbola shown in eq 5,

$$\Delta F=\frac{\Delta F_{\max}[\mathrm{L}]}{K_d+[\mathrm{L}]} \quad (5)$$

where F is the change in intrinsic fluorescence upon addition of ligand to enzyme, $F_{\max}$ is the maximum change in fluorescence at infinite ligand concentration, [L] is ligand concentration and K_{d} is the dissociation constant for the enzyme–ligand complex.

pH Studies

The pH dependency of the hPNMT-catalyzed reaction of PEA and AdoMet was measured over the range pH 6.0–10.0 at 30 °C in a buffer comprising ACES (100 mM) Tris (52 mM) and ethanolamine (52 mM). Across this pH range the buffer provides a constant ionic strength of 0.1 μM [44]. The reactions were carried out as described above and the kinetic parameters, k_{cat}, K_m^{PEA} and K_m^{AdoMet} were obtained by fitting initial rate data to eq 1. The pH dependency of inhibition by SK&F 29661 was also measured and K_i values obtained by fitting to eq 2. Data for the pH profiles were fitted to eq 6 or eq 7, as appropriate, using the computer programs of Cleland [45].

$$\log y = \log[C/(1+H/K_1+K_2/H)] \quad (6)$$

$$\log y = \log[C(1+H/K_1)/(1+H/K_2)(1+H/K_3)] \quad (7)$$

In equations 6 and 7, y represents k_{cat}, k_{cat}/K_m or $1/K_i$, C is the pH independent value of y, K_1, K_2 and K_3 are acid dissociation constants, and H is the proton concentration.

RESULTS

Initial Velocity Studies

The structures of the various substrates and inhibitors are provided in Figure 2. The hPNMT-catalyzed methylation of PEA has been shown previously to proceed in a linear manner [46]. Initial velocity patterns were obtained by varying the concentration of one substrate at different fixed concentrations of the other substrate. In each case the double-reciprocal plots intersected to the left of the vertical axis (data not shown), consistent with hPNMT operating by a sequential Bi Bi mechanism [47]. Data were fitted to eq 1 and the kinetic parameters for PEA, octopamine and 3-CF_3 PEA are summarized in Table 1.

The K_m values for octopamine and 3-CF_3-PEA were 20-fold and 200-lower, respectively, than that of PEA. Further, even though PEA had the highest value of k_{cat}, its k_{cat}/K_m value was an order of magnitude lower than those of the other two substrates. Conversely, the K_m values for AdoMet were similar with all three substrates.

Product and Dead-end Inhibition Studies

Product inhibition patterns were obtained with both AdoHcy and Epi. AdoHcy was found to be competitive against varied concentrations of AdoMet and non-competitive against PEA, whereas Epi was found to be non-competitive against both PEA and AdoMet. 7-Nitro THIQ was used as a dead-end analogue of PEA, and was found to be competitive against PEA as a substrate and uncompetitive against AdoMet (Figure 3). The inhibition data, provided in Table 2, are consistent with hPNMT operating by an ordered sequential mechanism with AdoMet binding before PEA.

Isothermal Titration Calorimetry Studies

The interaction of hPNMT with several substrates and inhibitors was examined by ITC and the data for binding of ligands to hPNMT are summarized in Table 3. A typical binding curve is shown in Figure 4 and, for all the ligands examined, the data fit best to a single-site model [43]. AdoMet and its product AdoHcy were found to bind to free hPNMT with dissociation constants (K_d) of 4.6 and 2.9 μM, respectively. Conversely, substrates such as PEA, NE, octopamine and 3-CF_3 PEA did not bind to free hPNMT, binding only being observed in the presence of AdoHcy. This provides further support for the suggestion that

hPNMT operates by an ordered mechanism with AdoMet binding first. Epi was also found bind to hPNMT in presence of either AdoMet or AdoHcy, although it did exhibit a 5-fold preference for the latter. The dead-end inhibitors SK&F 29661 and SK&F 64139 were found to bind to hPNMT in presence of AdoMet with K_d values similar to those obtained in initial velocity studies. Intriguingly, the tight-binding inhibitors SK&F 64139 and LY 134046 were also able to bind to free hPNMT (Table 3).

Fluorescence Studies

Fluorescence titrations were also employed to estimate the dissociation constants for enzyme-reactant complexes. The ligands were all found to quench the fluorescence emission of hPNMT, with a typical binding curve being shown in Figure 5. The K_d values obtained by this method (Table 4), were found to be comparable to those obtained by ITC and/or kinetic analysis.

pH Dependence of Kinetic Parameters

The pH dependence of the steady-state parameters was determined over the pH range of 6–10. The pH dependence of the K_i value for SK&F 29661 was determined over the same range. The pH-rate profiles are shown in Figure 6 and the data derived from them is shown in Table 5. The log$V$ profile is not simple, but appears to contain 3 pK_as, each of which causes partial inhibition when the group is protonated. The pK_i profile and the logV/K profiles are all bell shaped with slopes of unity on each side.

DISCUSSION

Methyltransferases show a diversity of kinetic mechanisms. For example, protoporphyrin methyltransferase operates by a ping pong mechanism [48] whereas bacterial glutamyl methyltransferase [49], DNA (cytosine) methyltransferase [50] and VP39, an mRNA cap-specific *O*-methyltransferase [51] all operate via a random sequential mechanism. In general, the small molecule methyltransferases such as guanidinoacetate *N*-methyltransferase [52], histamine *N*-methyltransferase [53], acetylserotinin *N*-methyltransferase [54] and glycine *N*-methyltransferase [55] have an ordered sequential mechanism, in which AdoMet binds first. By contrast, PNMT has been variously described as having mechanisms in which both substrates bound randomly [21], AdoMet bound first [18], or NE bound first [20].

Overall, the data described herein suggest that hPNMT operates by an ordered sequential mechanism at pH 8.0. An initial velocity pattern in which the lines intersect to the left of the y-axis on a double reciprocal plot is indicative of a sequential mechanism. This was seen for each of the three substrates examined (not shown). An ordered binding of substrates is suggested by inhibition studies with both reaction products and dead-end inhibitors. AdoHcy acts as a competitive inhibitor of AdoMet and as a non-competitive inhibitor of PEA, whereas Epi acts non-competitively with both substrates. Taken together this implies that the reaction is ordered and that AdoMet is the first substrate to bind [56]. This sequence is confirmed by studies using the dead-end inhibitor, 7-NO_2-THIQ. It was long thought that THIQ inhibitors such as SK&F 29661 and SK&F 64139 occupied the NE binding site and this was confirmed when the X-ray structures of the hPNMT:AdoHcy:octopamine [29] and hPNMT:AdoHcy:NE [32] complexes were determined. Therefore it was not a surprise when 7-NO_2-THIQ was found to be competitive with PEA. It was also found to be uncompetitive with AdoMet, confirming that AdoMet bound prior to PEA (Figure 3). The fact that Epi acted as a non-competitive inhibitor of PEA, the substrate it structurally mimics, indicates that Epi can bind to two forms of the enzyme [56]. The first is the form to which PEA binds,

i.e., the E:AdoMet complex. The second is likely to be the normal product complex, E:AdoHcy.

The kinetic studies provide dissociation constants for the E:AdoMet complex (K_{ia}) (Table 1) and for the E:AdoHcy complex (K_{ii} and K_{is}, Table 2), that are in the low micromolar range. Almost identical results are obtained with both ITC (Table 3) and fluorescence measurements (Table 4). In line with many small molecule methyltransferases [57], the K_d values for AdoMet and AdoHcy are quite similar. It has been suggested that the *in vivo* activity of many methyltransferases may be modulated by the intracellular [AdoMet] / [AdoHcy] ratio [58–60] and it would seem that hPNMT is no exception.

The above kinetic results suggested that Epi could bind to both the E:AdoMet and E:AdoHcy complexes. This prediction was confirmed by the ITC studies which showed Epi binding with K_d values of 23 and 4 μM, respectively. Indeed, all substrates tested were found to bind to the E:AdoHcy complex. That said, superposition of X-ray structures shows that the NE binding sites are virtually identical, regardless of whether AdoMet or AdoHcy is bound to the enzyme (not shown), so this may not be entirely unexpected. In fact, even when occupied only by phosphate (as in PDB ID 3KPJ) the NE binding site does not change. It is conceivable that, in addition to the [AdoMet] /[AdoHcy] ratio the intracellular [NE]/[Epi] ratio may also play a role in modulating the action of hPNMT. *In toto*, based on the kinetic and ligand binding studies, it would seem that the kinetic mechanism for hPNMT is the ordered sequential mechanism shown in Figure 7.

As shown in Figure 1A, the binding sites for both substrates are enclosed by a tight cover [27]. Moreover, to date, all X-ray structures of hPNMT have contained either AdoMet or AdoHcy. This (i) would suggest that a conformational change will be required for substrates to enter the hPNMT active site, and (ii) is consistent with an ordered mechanism with AdoMet binding first. Prior to this study, hints of an ordered mechanism for hPNMT were provided by a kinetic analysis which showed that the binding of inhibitors such as SK&F 29661 and 7-nitro THIQ was enhanced ~50-fold in the presence of AdoMet [30]. In the present study, attempts to determine a K_i value for SK&F 29661 in the absence of AdoMet or AdoHcy were unsuccessful. Conversely, the inhibitors with K_i values in the low nanomolar range, SK&F 64139 and LY 134046 (Table 1), were able to bind to the enzyme in the absence of AdoMet or AdoHcy. This was demonstrated by both ITC and fluorescence experiments and, for both inhibitors, the K_d value obtained for binding to the free enzyme was significantly (i.e., >100-fold) greater that that obtained for binding to hPNMT in the presence of AdoMet. On that basis it would appear that (i) the two inhibitors are able to access a binding site on the enzyme, (ii) the binding site is not optimal, and (iii) binding of the co-substrate (or product) greatly improves the binding of the inhibitor. However, in the absence of structural information, we cannot say whether the inhibitor occupies the same binding site on the free enzyme as it does in the enzyme:substrate or enzyme:product complex. Further, based on kinetic data [30], SK&F 29661 should bind to the free enzyme with a K_i value around 6 μM but we saw no evidence of its binding, even at concentrations up to the 25 μM used in these experiments. On the other hand, LY 134046 binds to the hPNMT:AdoMet complex ~30 times more tightly than SK&F 29661 (Table 1). Accordingly, based on the data in Tables 3 and 4 for the binding of LY 134046 to the free enzyme, SK&F 29661 may be expected to bind to the free enzyme with a K_i value of ca. 130 μM. On that basis it is not surprising that we found no evidence of binding at 25 μM.

The NE binding site shows four ionizable residues that interact with NE (Figure 1B). Using the structure of hPNMT in which NE has been replaced by phosphate (PDB ID 3KPJ), the PROPKA program [61, 62] predicts that the sidechains of Lys57, Glu185, Glu219 and Asp267 will have pK_a values of 7.53, 7.33, 9.59 and 4.19, respectively. An earlier study

showed that the k_{cat} value of the K57A variant was unchanged, and the reduction in k_{cat} shown by the D267A variant was attributed to the inability of that variant to correctly position the sidechain for catalysis [30]. Thus, and in accord with the computational studies, it would seem that the pK_as of two glutamate residues, 7.33 and 9.59, are likely to appear in the pH-rate profiles.

The plot of log*V* versus pH (Figure 6A) is not simple. Although fitting to eq 7 provides 3 p*K*s (Table 5), it is also conceivable that the plot represents 2 p*K*s. The p*K* at ~9 causes partial inhibition when the group is protonated and the second, at ~7, that causes further loss of activity (W.W. Cleland, personal communication). Superficially, based on the PROPKA results, the higher pK_a could be attributed to Glu219, and the lower to Glu185.

The plot of log*V/K* for PEA is bell-shaped indicating that a protonated and an unprotonated group are required for catalysis. Two pK_as, of 8.66 and 9.26, were derived using eq 6. The pK_a of the side chain nitrogen of PEA is calculated to be 8.4 (Advanced Chemistry Development Software; SciFinder). For a S_N2 reaction to take place, this nitrogen needs to be deprotonated so, potentially, is represented by the lower pK_a in the log*V/K* profile. The log*V/K* versus pH plot for AdoMet is also bell-shaped. Once again the higher pK_a is similar to that calculated for Glu219 but the second value, 7.25, is almost 1.5 pH units lower than that seen in the PEA profile. Unlike the latter, AdoMet does not possess any ionizable residues with pK_a values in this range, so this lower value could be ascribed to Glu185.

The pK_i versus pH plot for the THIQ inhibitor, SK&F 29661, suggests that both protonation and deprotonation will reduce binding affinity, with pK_as of 8.48 and 9.08 being derived using eq 6. In addition, the pK_a of the ring nitrogen of SK&F 29661 was determined to be 8.5 by pH titration (data not shown). As there is some evidence that THIQ inhibitors prefer to bind in their neutral form [16], it is not unreasonable to attribute the observed pK_a of 8.48 to the inhibitor as protonation of this group leads to a loss of activity. It is notable that in all of the plots, a pK_a of ~9 is observed. It is feasible that this belongs to the same group on the enzyme, probably Glu219. However, one of the problems with interpreting this data is that the observed pK_a values are relatively close together. Cook and Cleland [56] caution that in such cases the pH profile does not distinguish between which group must be protonated or which group must be deprotonated for optimal activity.

In summary, these experiments have clearly demonstrated that hPNMT operates by an ordered sequential mechanism, with AdoMet binding first. Further, it would appear that one of the groups in the *V/K* profile is related to substrate binding as it does not appear in the *V* profile. However, interpretation of the pH data is not so straightforward and, most likely, will necessitate additional experiments in which the pK_as of the ionizable groups are perturbed through mutagenesis.

Acknowledgments

This work was supported, in part, by the National Institutes of Health (NIH HL 34193). We thank Prof. Paul F. Cook (University of Oklahoma) and Prof. W. W. Cleland (University of Wisconsin) for 14 helpful advice and discussions on data treatment and analysis. W.W. “Mo” Cleland was a friend and mentor, and this manuscript is dedicated to his memory.

Abbreviations

hPNMT	human phenylethanolamine *N*-methyltransferase
AdoMet	S-adenosyl-L-methionine

AdoHcy	S-adenosyl-L-homocysteine
NE	norepinephrine
Epi	epinephrine
ITC	isothermal titration calorimetry
PEA	phenylethanolamine
THIQ	tetrahydroisoquinoline

References

1. Kirshner N, Goodall M. Biochim Biophys Acta. 1957; 24:658–659. [PubMed: 13436503]
2. Axelrod J. J Biol Chem. 1962; 237:1657–1660. [PubMed: 13863458]
3. Fuller, RW. Epinephrine in the Central Nervous System. Stolk, JM.; U'Prichard, DC.; Fuxe, K., editors. Oxford University Press; New York: 1988. p. 366-369.
4. Hokfelt T, Fuxe K, Goldstein M, Johannson O. Brain Res. 1974; 66:235–251.
5. Black J, Waeber B, Bresnahan MR, Gavras I, Gavras H. Circ Res. 1981; 49:518–524. [PubMed: 7249286]
6. Crowley WR, Terry LC, Johnson MD. Endocrinology. 1982; 110:1102–1107. [PubMed: 7037366]
7. Stone EA, Grunewald GL, Lin Y, Ahsan R, Rosengarten H, Kramer HK, Quartermain D. Synapse. 2003; 49:67–76. [PubMed: 12710017]
8. Burke WJ, Chung HD, Huang JS, Huang SS, Haring JH, Strong R, Marshall GL, Joh TH. Ann Neurol. 1988; 24:532–536. [PubMed: 3239955]
9. Burke WJ, Galvin NJ, Chung HD, Stoff SA, Gillespie KN, Cataldo AM, Nixon RA. Brain Res. 1994; 661:35–42. [PubMed: 7834382]
10. Fuller RW, Mills J, Marsh MM. J Med Chem. 1971; 14:322–325. [PubMed: 5553744]
11. Fuller RW, Roush BW, Snoddy HD, Molloy BB. J Med Chem. 1973; 16:106–109. [PubMed: 4683104]
12. Kaiser C, Pendleton RG. Intra-Science Chem Rept. 1974; 8:43–55.
13. Fuller RW, Molley BB. Biochem Pharmacol. 1977; 26:446–447. [PubMed: 849338]
14. Fuller RW, Hemrick-Luecke S, Toomey RE, Horng JS, Ruffolo RR Jr, Molloy BB. Biochem Pharmacol. 1981; 30:1345–1352. [PubMed: 6268095]
15. Bondinell WE, Chapin FW, Frazee JS, Girard GR, Holden KG, Kaiser C, Maryanoff C, Perchonock CD, Gessner GW, Hieble JP, et al. Drug Metab Rev. 1983; 14:709–721. [PubMed: 6352222]
16. Grunewald GL, Caldwell TM, Li Q, Criscione KR. J Med Chem. 1999; 42:3315–3323. [PubMed: 10464018]
17. Grunewald GL, Romero FA, Criscione KR. J Med Chem. 2005; 48:1806–1812. [PubMed: 15771426]
18. Pendleton RG, Snow IB. Mol Pharmacol. 1973; 9:718–725. [PubMed: 4762633]
19. Lee HS, Schulz AR, Fuller RW. Arch Biochem Biophys. 1978; 185:239–250. [PubMed: 623487]
20. Pohorecky LA, Baliga BS. Biochem Pharmacol. 1972; 21:2859–2866. [PubMed: 4646806]
21. Connet RJ, Kirshner N. J Biol Chem. 1970; 245:329–334. [PubMed: 5412063]
22. Kitabchi AE, Williams RH. Bichimica et Biophysica Acta. 1969; 178:181–184.
23. Caine JM, Macreadie IG, Grunewald GL, McLeish MJ. Prot Express Purif. 1996; 8:160–166.
24. Grunewald GL, McLeish MJ, Criscione KR. Bioorg Med Chem Lett. 2001; 11:1579–1582. [PubMed: 11412985]
25. Wu Q, Criscione KR, Grunewald GL, McLeish MJ. Bioorg Med Chem Lett. 2004; 14:4217–4220. [PubMed: 15261273]

26. Begun J, McLeish MJ, Caine JM, Palant E, Grunewald GL, Martin JL. Acta Crystallogr Sect D: Biol Crystallogr. 2002:314–315. [PubMed: 11807261]
27. Martin JL, Begun J, McLeish MJ, Caine JM, Grunewald GL. Structure. 2001; 9:977–985. [PubMed: 11591352]
28. McMillan FM, Archbold J, McLeish MJ, Caine JM, Criscione KR, Grunewald GL, Martin JL. J Med Chem. 2004; 47:37–44. [PubMed: 14695818]
29. Gee CL, Tyndall JDA, Grunewald GL, Wu Q, McLeish MJ, Martin JL. Biochemistry. 2005; 44:16875–16885. [PubMed: 16363801]
30. Wu Q, Gee CL, Lin F, Tyndall JD, Martin JL, Grunewald GL, McLeish MJ. J Med Chem. 2005; 48:7243–7252. [PubMed: 16279783]
31. Gee CL, Drinkwater N, Tyndall JD, Grunewald GL, Wu Q, McLeish MJ, Martin JL. J Med Chem. 2007; 50:4845–4853. [PubMed: 17845018]
32. Drinkwater N, Gee CL, Puri M, Criscione KR, McLeish MJ, Grunewald GL, Martin JL. Biochem J. 2009; 422:463–471. [PubMed: 19570037]
33. Martin JL, McMillan FM. Curr Opin Struct Biol. 2002; 12:783–793. [PubMed: 12504684]
34. Schubert HL, Blumenthal RM, Cheng X. Trends Biochem Sci. 2003; 28:329–335. [PubMed: 12826405]
35. Fuller RW, Hunt JM. Life Sci. 1967; 6:1107–1112. [PubMed: 6033048]
36. Deguchi T, Barchas J. J Biol Chem. 1971; 246:3175–3181. [PubMed: 5574392]
37. Lee HS, Schulz AR, Fuller RW. Arch Biochem Biophys. 1978; 185
38. Georgieva P, Wu Q, McLeish MJ, Himo F. BBA - Proteins and Proteomics. 2009; 1794:1831–1837. [PubMed: 19733262]
39. Hou QQ, Wang JH, Gao J, Liu YJ, Liu CB. Biochim Biophys Acta. 2012; 1824:533–541. [PubMed: 22326747]
40. Romero FA, Vodonick SM, Criscione KR, McLeish MJ, Grunewald GL. J Med Chem. 2004; 47:4483–4493. [PubMed: 15317460]
41. Cleland WW. Biochim Biophys Acta. 1963; 67:104–137. [PubMed: 14021667]
42. Bradford MM. Anal Biochem. 1976; 72:248–254. [PubMed: 942051]
43. Wiseman T, Williston S, Brandts JF, Lin LN. Anal Biochem. 1989; 179:131–137. [PubMed: 2757186]
44. Ellis KJ, Morrison JF. Methods Enzymol. 1982; 87:405–426. [PubMed: 7176924]
45. Cleland WW. Methods Enzymol. 1979; 63:103–138. [PubMed: 502857]
46. Wu Q, Caine JM, Thomson SA, Slavica M, Grunewald GL, McLeish MJ. Bioorg Med Chem Lett. 2009; 19:1071–1074. [PubMed: 19171483]
47. Cleland WW. Adv Enzymol Relat Areas Mol Biol. 1977; 45:273–387. [PubMed: 21524]
48. Yee WC, Eglsaer SJ, Richards WR. Biochem Biophys Res Commun. 1989; 162:483–490. [PubMed: 2751667]
49. Simms SA, Subbaramaiah K. J Biol Chem. 1991; 266:12741–12746. [PubMed: 2061337]
50. Sano H, Noguchi H, Sager R. Eur J Biochem. 1983; 135:181–185. [PubMed: 6884360]
51. Barbosa E, Moss B. J Biol Chem. 1978; 253:7698–7702. [PubMed: 701282]
52. Takata Y, Konishi K, Gomi T, Fujioka M. Journal of Biological Chemistry. 1994; 269:5537–5542. [PubMed: 8119887]
53. Horton JR, Sawada K, Nishibori M, Zhang X, Cheng X. Structure. 2001; 9:837–849. [PubMed: 11566133]
54. Morton DJ, Kock N. J Pineal Res. 1990; 8:35–40. [PubMed: 2338611]
55. Konishi K, Fujioka M. Biochemistry. 1987; 26:8496–8502. [PubMed: 3442671]
56. Cook, PF.; Cleland, WW. Enzyme Kinetics and Mechanism. Garland Science; New York: 2007.
57. Fujioka M. Int J Biochem. 1992; 24:1917–1924. [PubMed: 1473604]
58. Kerr SJ, Heady JE. Adv Enzyme Regul. 1974; 12:103–117. [PubMed: 4376890]
59. Cantoni, GL.; CPK. Natural sulfur compounds: novel biochemical and structural aspects. Cavallini, D.; Gaulli, GE.; ZV, editors. Plemun Press; New York: 1980. p. 67-80.

60. Herrmann W, Schorr H, Obeid R, Makowski J, Fowler B, Kuhlmann MK. Clin Chem. 2005; 51:891–897. [PubMed: 15774574]
61. Li H, Robertson AD, Jensen JH. Prot Struct Funct Bioinf. 2005; 61:704–721.
62. Bas DC, Rogers DM, Jensen JH. Prot Struct Funct Bioinf. 2008; 73:765–783.
63. Taylor, JR. An introduction to error analysis. University Science Books; Sausalito, CA: 1997.
64. The PyMOL Molecular Graphics System, Version 1.4. Schrödinger, LLC; http://www.pymol.org

Highlights

- hPNMT operates by an ordered mechanism with AdoMet binding before norepinephrine.
- Epinephrine and AdoHcy both showed evidence of product inhibition.
- THIQ inhibitors compete with phenylethanolamine but are uncompetitive with AdoMet.
- Binding of AdoMet increased the binding affinity of the second substrate/inhibitor.
- log*V/K* pH profiles are all bell shaped with slopes of unity on each side.

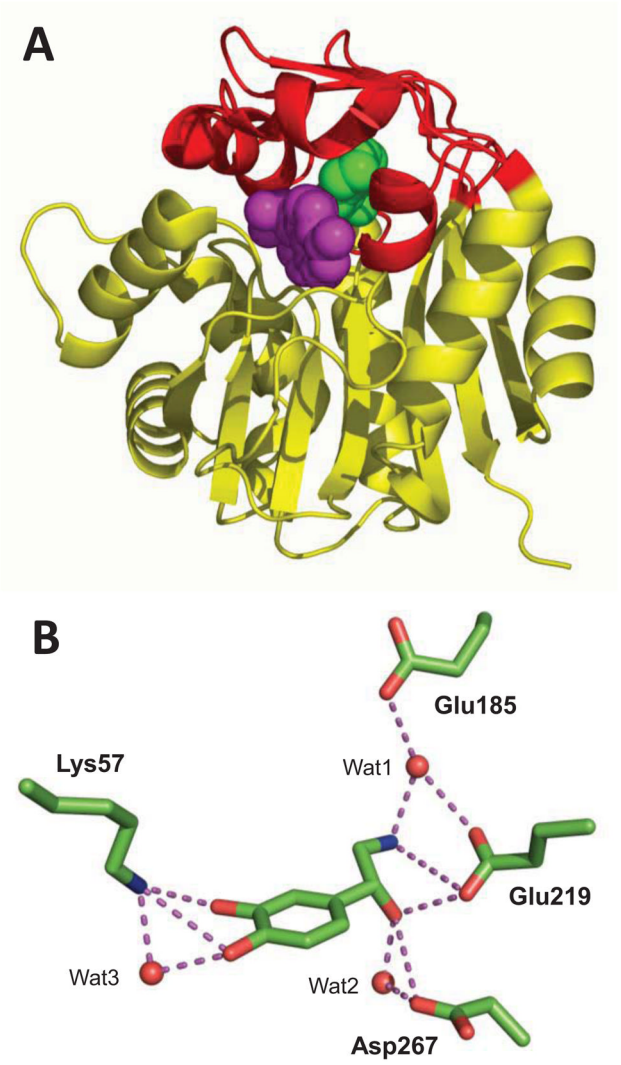

Figure 1.
(A) Structure of hPNMT in complex with AdoHcy (magenta) and SK&F 29661 (green). The "cap" over the active site is in red. This figure was generated with PyMOL [64] using the coordinates from the PDB entry, 1HNN. (B) Interaction of NE with ionizable residues in the active site. Dotted lines indicate a distance of <3.5 Å. Figure based on PDB ID 3HCD.

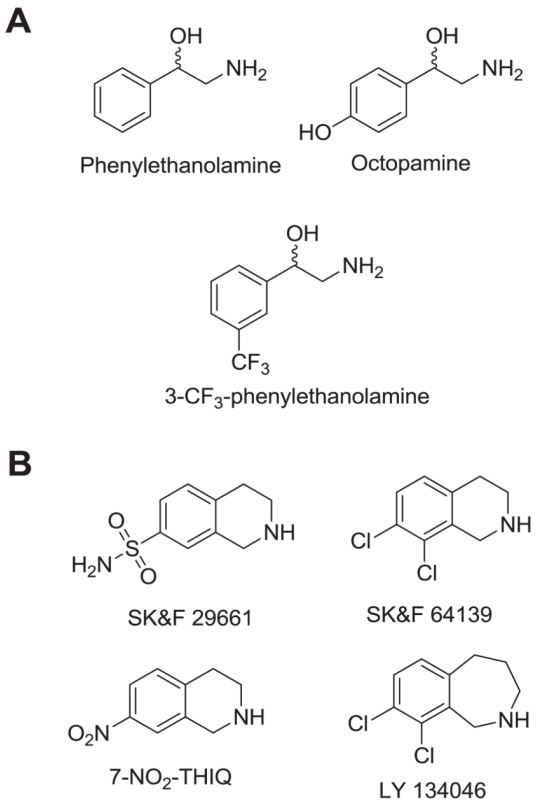

Figure 2.
Structures of hPNMT (A) substrates and (B) inhibitors used in this study.

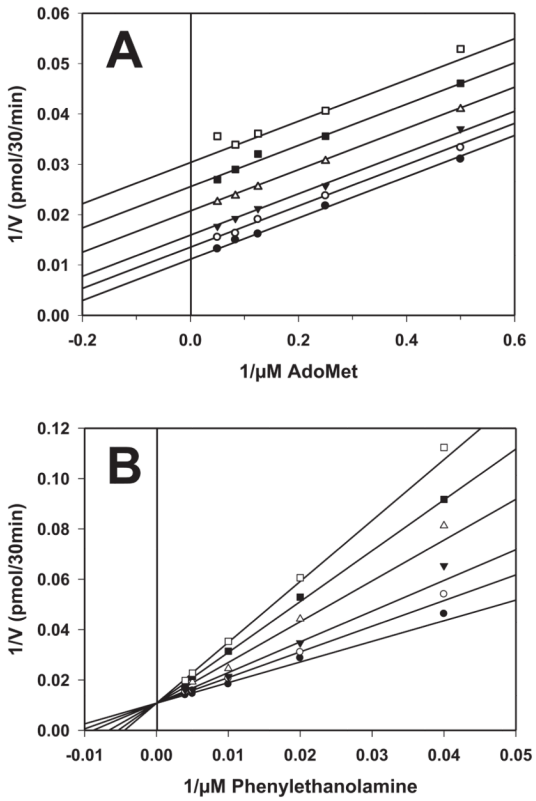

Figure 3.

Dead-end inhibition of hPNMT by 7-NO_2-THIQ. The inhibition reactions were carried out at 30 °C in 50 mM potassium phosphate buffer (pH 8.0). (A) The PEA concentration was held at 100 μM. (B) The AdoMet concentration was 5 μM. In both cases the 7-NO_2-THIQ concentrations were 0 (●), 20 (○), 40 (▼), 80 (△), 120 (■) and 160 nM (□). The lines represent fits of the data to eq 4 and 2, respectively.

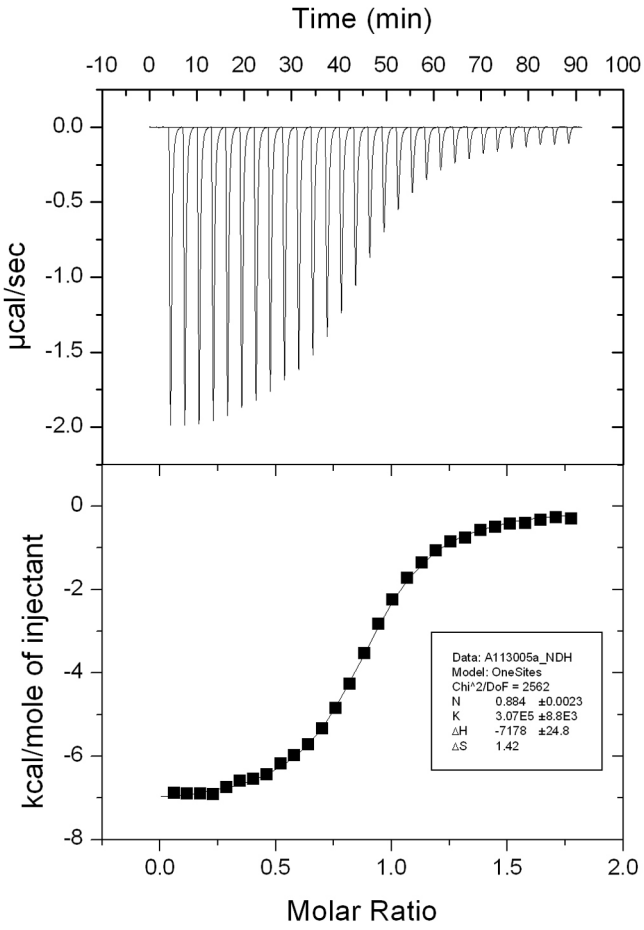

Figure 4.

Isothermal titration calorimetry (ITC) analysis of binding of AdoMet to hPNMT. The reaction was carried at room temperature. The cell contained 25 μM hPNMT in 50 mM KPO_4 at pH 8.0 and the syringe contained 500 μM AdoMet in the same buffer. A total of 25 injections were made at 180 sec intervals. (Top panel) Raw ITC data. (Bottom panel) Data for the integrated heat pulses, normalized per mol of injectant as a function of the molar ratio ([AdoMet]/[hPNMT]). The binding curve (solid line) was best fit to a 1 site model (inset).

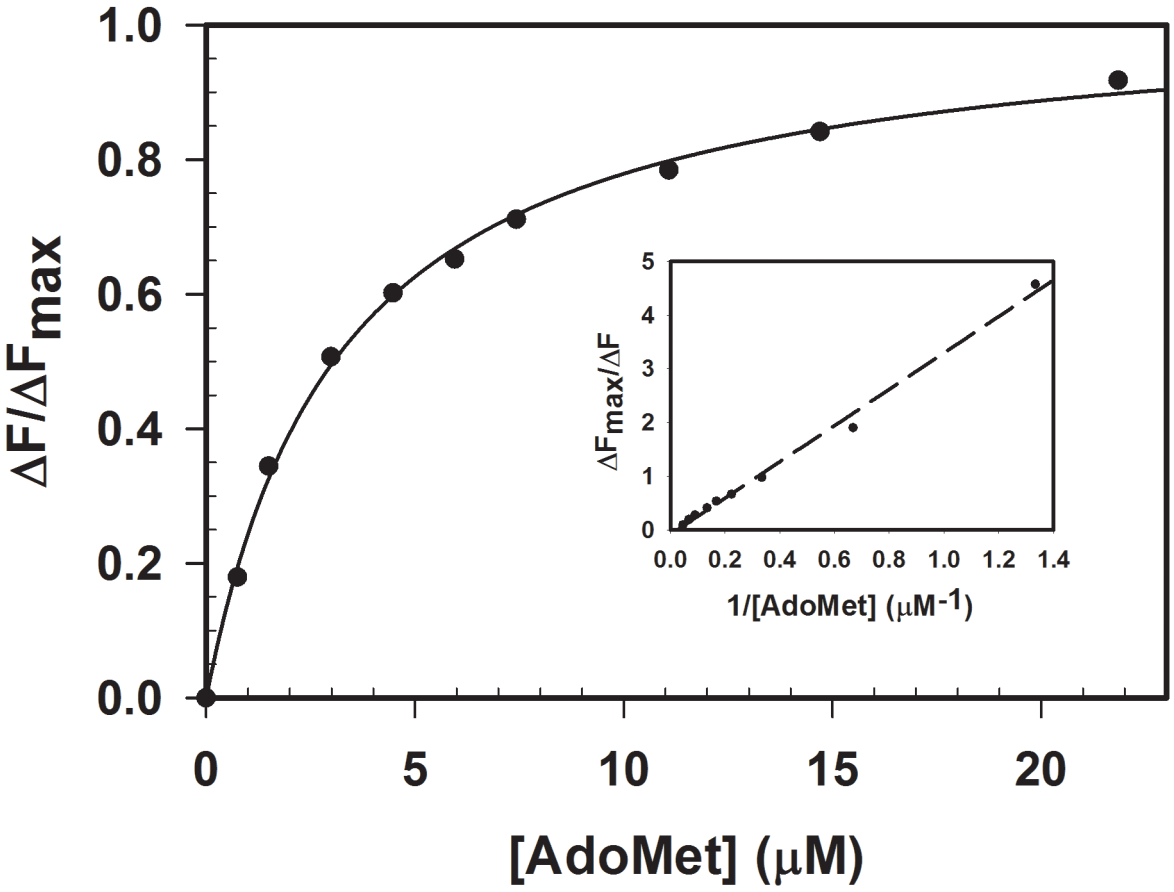

Figure 5.
Fluorescence binding curve for the interaction of AdoMet with hPNMT. Data recorded at λ_{ex} 280 nm and λ_{em} 348 nm were used in the analysis. The solid line represents the fit of the data to eq 5 and provides a K_d of 3.3±0.2 μM. The double reciprocal plot (inset) provides a K_d of 3.4±0.1 μM.

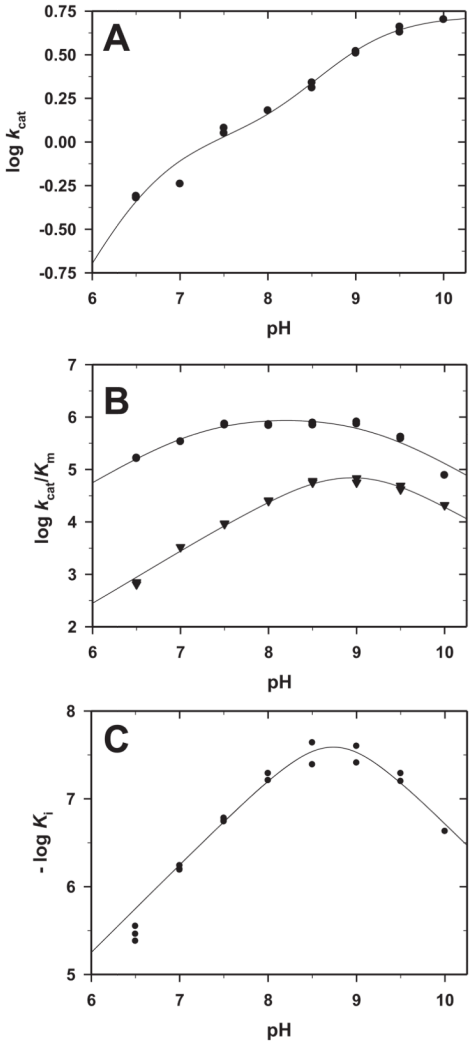

Figure 6.
pH dependence of the kinetic parameters (A) k_{cat}; (B) k_{cat}/K_m for AdoMet (●) and PEA (▼); and (C) K_i for SK&F 29661. The data points are the experimentally determined values at 30 °C while the lines are theoretical based to fits of the data using eq 7 for A and eq 6 for B and C.

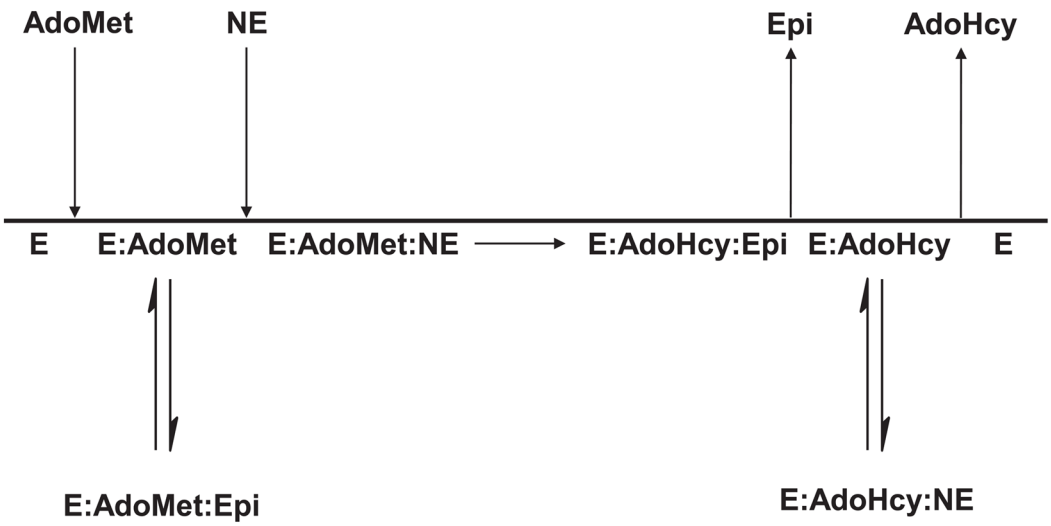

Figure 7.
Proposed kinetic mechanism for reaction of hPNMT with norepinephrine and S-adenosyl-Lmethionine.

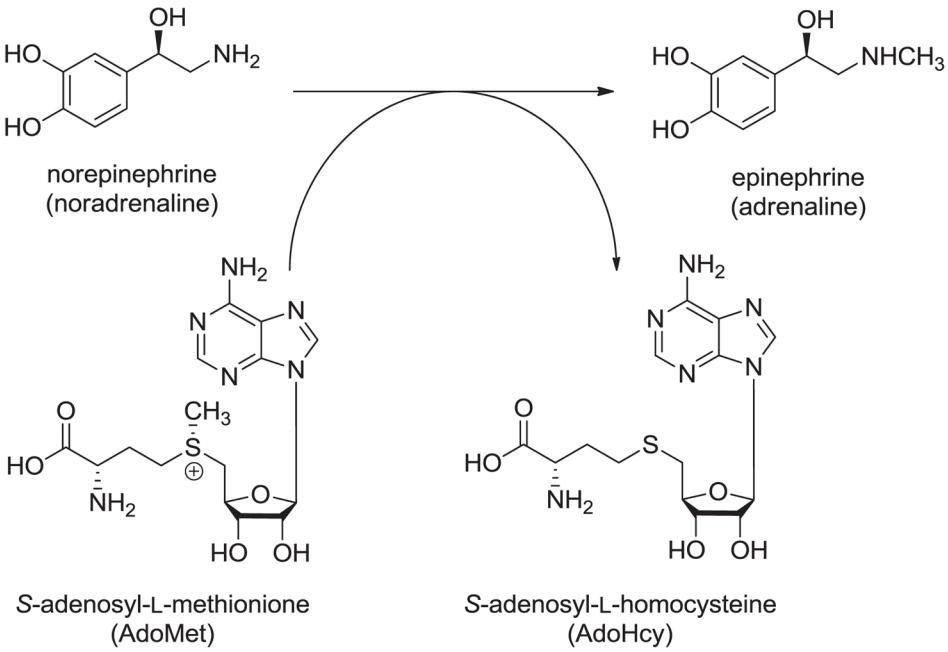

Scheme 1.
Reaction catalyzed by hPNMT

Table 1

Summary of kinetic parameters for PNMT with substrates/inhibitors[a]

Substrate/inhibitor	K_a (μM)	K_b (μM)	K_{ia} (μM)	k_{cat} (min^{-1})	k_{cat}/K_a (M^{-1} min^{-1})[b]	K_i (nM)
(±)-PEA[c]	100 ± 4	3.4 ± 0.2	180 ± 8	2.84 ± 0.10	(2.8 ± 0.2) × 10^4	
(±) Octopamine	5.5 ± 1.0	6.7 ± 0.3	2.1 ± 0.2	1.23 ± 0.05	(2.2 ± 0.4) × 10^5	
(±) 3-CF_3 PEA	0.54 ± 0.10	1.2 ± 0.4	2.4 ± 0.7	0.50 ± 0.01	(9.3 ± 1.7) × 10^5	
SK&F 64139						1.6 ± 0.2[c]
LY 134046						4.4 ± 1.1[c]
7-NO_2THIQ						78 ± 14[c]
SK&F 29661						120 ± 20[c]

[a] Reactions were carried out in phosphate buffer, pH 8.0 at 30 °C. Both substrate concentrations were varied between 0.3–3×K_m. Initial velocity data were fit to eq 1. K_b is the Michaelis constant for AdoMet.

[b] Error in k_{cat}/K_m value determined using propagation of error formaula as described in reference [63]

[c] Data from reference [30]

Table 2

Kinetic constants for product and dead-end inhibitors of hPNMT[a]

Inhibitor	Varied Substrate	Fixed substrate[a]	Inhibition pattern	K_{is} (μM)	K_{ii} (μM)
AdoHcy	PEA	AdoMet	NC[b]	2.5 ± 0.28	1.0 ± 0.02
AdoHcy	AdoMet	PEA	C[c]	0.8 ± 0.04	
Epinephrine	PEA	AdoMet	NC[b]	20 ± 0.2	51 ± 1.0
Epinephrine	AdoMet	PEA	NC[b]	71 ± 9.5	22 ± 0.8
7-NO_2THIQ	PEA	AdoMet	C[c]	0.09 ± 0.01	
7-NO_2THIQ	AdoMet	PEA	U[d]		0.08 ± 0.005

[a] Reactions were carried out in phosphate buffer, pH 8.0 at 30 °C. One substrate concentration was varied between 0.4–3×K_m while the other, either AdoMet or PEA, was held constant at 5 μM or 100 μM, respectively. The inhibitor was varied between 0–2.5×K_i.

[b] Initial velocity data were fit to eq 3.

[c] Initial velocity data were fit to eq 2.

[d] Initial velocity data were fit to eq 4.

Table 3

Dissociation constants for ligand-hPNMT complexes from isothermal titration calorimetry[a]

Varied Ligand	Fixed ligand	K_d (varied ligand) (μM)
AdoMet	–	4.6 ± 0.7
AdoHcy	–	2.9 ± 0.9
Epi	AdoHcy	4.1 ± 0.7
Epi	AdoMet	23 ± 2.5
NE	AdoHcy	7.2 ± 0.2
3-CF_3-PEA	AdoHcy	1.2 ± 0.3
PEA	AdoHcy	60 ± 2
Octopamine	AdoHcy	3.3 ± 0.1
SK&F 29661	AdoMet	0.19 ± 0.01
SK&F 29661	AdoHcy	7.4 ± 2.3
SK&F 29661	-	n.d.[b]
SK&F 64139	–	0.42 ± 0.03
SK&F 64139	AdoMet	0.004 ± 0.001
LY 134046	–	3.2 ± 0.2

[a] Binding studies were carried out at out as described in materials and methods. Data were fit to a one site model.

[b] No evidence observed for inhibitor binding up to 25 μM

Table 4

Dissociation constants for ligand-hPNMT complexes from fluorescence titration[a]

Varied Ligand	Fixed Ligand	K_d (μM)
AdoMet	–	3.3 ± 0.2
AdoHcy	–	4.3 ± 0.7
SK&F 29661	AdoHcy	1.1 ± 0.2
SK&F 64139	–	0.88 ± 0.15
LY 134046	–	5.5 ± 0.4

[a]Fluorescence data (λ_{ex} 280 nm; λ_{em} 348 nm) were collected at room temperature. Dissociation constants were obtained by fitting data to eq 5.

Table 5

Data from pH-rate profiles

	pK_a1	pK_a2	pK_a3
LogV^a	6.63 ± 0.28	8.23 ± 0.36	8.93 ± 0.32
LogV/K_{PEA}[b]	–	8.66 ± 0.03	9.26 ± 0.03
LogV/K_{AdoMet}[b]	–	7.25 ± 0. 12	9.15 ± 0.12
p$K_{i\ SK\&F\ 29661}$[b]	–	8.48 ± 0.04	9.08 ± 0.04

[a] pK_a values obtained by fitting to eq 7.

[b] pK_a values obtained by fitting to eq 6.